

Azimuthal asymmetry in $J/\psi + \gamma$ and $J/\psi + J/\psi$ production in ultraperipheral heavy-ion collisions at LHC

Yu Jia ^{*,1} Wen-Long Sang ^{†,2} Xiaonu Xiong ^{‡,3} Jian Zhou ^{§,4,5} and Ya-jin Zhou ^{¶,4}

¹*Institute of High Energy Physics, Chinese Academy of Sciences, Beijing 100049, China*

²*School of Physical Science and Technology, Southwest University, Chongqing 400700, China*

³*School of Physics and Electronics, Central South University, Changsha 410083, China*

⁴*Key Laboratory of Particle Physics and Particle Irradiation (MOE),
Institute of Frontier and Interdisciplinary Science,
Shandong University, (QingDao), Shandong 266237, China*

⁵*Southern Center for Nuclear-Science Theory (SCNT), Institute of Modern Physics,
Chinese Academy of Sciences, HuiZhou, Guangdong 516000, China*

(Dated: December 30, 2025)

Two-photon collision in ultraperipheral heavy-ion collisions (UPCs) provides a unique and powerful platform for probing QCD with linearly polarized quasi-real photons. While photon polarization effects have been recognized in dilepton and even in light hadrons production, their consequences for heavy quarkonium production remain unexplored. In this work we investigate for the first time the $\gamma\gamma \rightarrow J/\psi + \gamma(J/\psi)$ channels in Pb-Pb UPCs at the Large Hadron Collider (LHC), by integrating the non-relativistic QCD (NRQCD) factorization approach with the transverse-momentum-dependent (TMD) photon distributions. Based on the helicity amplitudes at lowest order in strong coupling and velocity expansion, we predict sizable $\cos(2\phi)$ and $\cos(4\phi)$ azimuthal asymmetries arising from the interference of linearly polarized photon states. These azimuthal-dependent observables, defined as the ratios of weighted to unweighted cross sections, are expected to be stable against including the higher-order radiative corrections and varying nonperturbative NRQCD matrix elements, thus offering a fresh test of quarkonium production mechanism and the photon TMD structure in the ultrarelativistic limit.

I. INTRODUCTION

Ultraperipheral heavy-ion collisions (UPCs) at the Large Hadron Collider (LHC) and Relativistic Heavy Ion Collider (RHIC) generate intense electromagnetic fields that serve a potent source of quasi-real photons. These coherently emitted photons are linearly polarized along the direction of their transverse momentum, a property that can induce significant azimuthal asymmetries in final-state particle distributions. A prominent example is the sizable $\cos(4\phi)$ modulation observed by the STAR collaboration in the Breit-Wheeler process $\gamma\gamma \rightarrow l^+l^-$ [1], with further investigations carried out by ALICE [2–5], CMS [6], ATLAS [7], and STAR [8]. These measurements underscore the potential of utilizing linearly polarized photons to probe Quantum Chromodynamics (QCD) and Quantum Electrodynamics (QED) in a clean environment, largely free from hadronic background [9, 10]. This has stimulated broad theoretical interest in two-photon processes, ranging from studies of QED in extreme conditions [11–42] and searches for new

physics [43, 44]¹.

Numerous proposals has been advocated to extracting the gluon TMDs through azimuthal asymmetries in high energy pp collisions [45–62], among which the associated heavy quarkonium production with a photon, *e.g.*, $gg \rightarrow J/\psi + \gamma + X$, stands out as a clean probe, partly due to clean experimental signature of J/ψ and photon [63, 64], partly because the colorless final state minimizes final-state interactions [65, 66].

Somewhat surprisingly, despite the great experimental and theoretical cleanliness, the azimuthal asymmetry in simpler cousin process $\gamma\gamma \rightarrow J/\psi + \gamma$ in UPCs, and the impact of the photon linear polarization, has never been explored in literature. To date existing studies of exclusive heavy quarkonium production channels in UPCs, exemplified by $\gamma\gamma \rightarrow J/\psi + \gamma(J/\psi)$ [62, 67–73], have predominantly relied on the *equivalent photon approximation* (EPA), which is essentially equivalent to QED collinear factorization, combined with non-relativistic QCD (NRQCD) factorization approach [74]. By inherently averaging over the transverse polarization of the incoming photons, the EPA approach is unable

^{*}jiay@ihep.ac.cn

[†]wlsang@swu.edu.cn

[‡]xnxiong@csu.edu.cn

[§]jzhou@sdu.ac.cn

[¶]zhouyj@sdu.ac.cn

¹ It is worth mentioning that, a recent preliminary study of STAR Collaboration has reported the observation of light hadron pair production in UPCs, *viz.*, $\gamma\gamma \rightarrow p\bar{p}$. For some theoretical analysis, see Refs. [33, 34].

to capture the azimuthal modulations driven by the interference of helicity states, thus leaving a gap in our understanding of quarkonium production mechanisms in the TMD regime.

The aim of this paper is to bridge this gap by combining the QED TMD factorization with the NRQCD approach to account for the photon-induced quarkonium production of $J/\psi + \gamma(J/\psi)$ in UPCs. Our input is the helicity amplitudes for $\gamma\gamma \rightarrow J/\psi + \gamma(J/\psi)$ at lowest-order (LO) in the charm quark velocity, v , and QCD coupling constant α_s . We present the predictions for $\cos(2\phi)$ and $\cos(4\phi)$ azimuthal asymmetries, which are direct consequences of the linear polarization of the incoming quasi-real photons. Under realistic LHC kinematic conditions, we find that these asymmetries are sizable with cross sections large enough to yield a significant number of events per run. Furthermore, we anticipate that these predicted polarization observables, defined as ratios of weighted to unweighted cross sections, are theoretically stable against uncertainties in NRQCD long-distance matrix elements (LDMEs) and including the higher order radiative and relativistic corrections. This work may provide a novel window of testing the exclusive quarkonium production mechanism.

II. $J/\psi + \gamma(J/\psi)$ PRODUCTION IN UPCS

The exclusive production of $J/\psi + \gamma(J/\psi)$ in UPCs is mediated by two-photon collision, with both nuclei remain intact. Let us specialize to the reactions $\text{Pb} + \text{Pb} \rightarrow \text{Pb} + \text{Pb} + J/\psi + \gamma(J/\psi)$. The kinematics of the partonic subprocesses is specified by

$$\gamma(x_1 P + k_{1\perp}) + \gamma(x_2 \bar{P} + k_{2\perp}) \rightarrow J/\psi(p_1) + \gamma(J/\psi)(p_2), \quad (1)$$

where $x_1 P$ and $x_2 \bar{P}$ represent the longitudinal momenta of two incoming photons, and $k_{1,2\perp} = (0, 0, \mathbf{k}_{1,2\perp})$ signify the corresponding transverse momenta of incoming photons. The representative lowest-order Feynman diagrams for these partonic reactions are depicted in Fig. 1.

As mentioned before, the quasi-real photons emitted from the relativistic lead ions are linearly polarized, with the polarization vectors aligned with their transverse momenta $\mathbf{k}_{1,2\perp}$. Consequently, to access the azimuthally-dependent observables in the correlation limit, one ought to utilize the TMD factorization approach, rather than the standard collinear factorization approach widely used in the preceding studies in two-photon physics. To this end, it is convenient to introduce two additional transverse momenta variables: $\mathbf{P}_\perp \equiv \frac{\mathbf{p}_{1\perp} - \mathbf{p}_{2\perp}}{2}$, and $\mathbf{q}_\perp \equiv \mathbf{p}_{1\perp} + \mathbf{p}_{2\perp} = \mathbf{k}_{1\perp} + \mathbf{k}_{2\perp}$. The azimuthal angle is defined by $\cos\phi \equiv \mathbf{P}_\perp \cdot \hat{\mathbf{q}}_\perp$. In the correlation limit with $|\mathbf{q}_\perp| \ll |\mathbf{P}_\perp|$, it is legitimate to approximate $\mathbf{P}_\perp \approx \mathbf{p}_{1\perp} \approx -\mathbf{p}_{2\perp}$.

To incorporate both the impact parameter \mathbf{b}_\perp and the \mathbf{q}_\perp dependence simultaneously, one can derive the

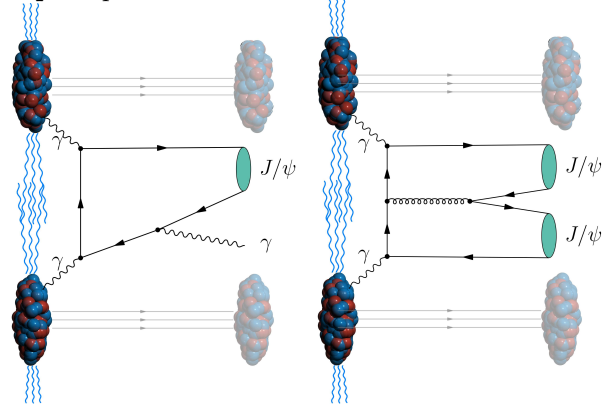


FIG. 1: Representative lowest-order diagrams for $\gamma\gamma \rightarrow J/\psi + \gamma(J/\psi)$ (left) and $\gamma\gamma \rightarrow J/\psi + J/\psi$ (right).

differential cross section for the associated $J/\psi + \gamma(J/\psi)$ production, following the formalism originally developed in Refs. [75, 76], which is valid in the correlation limit. After some manipulation, we cast the azimuthal-dependent differential cross section in the following convolutional form [77]:

$$\begin{aligned} \frac{d\sigma}{d^2\mathbf{p}_{1\perp} d^2\mathbf{p}_{2\perp} dy_1 dy_2 d^2\mathbf{b}_\perp} &= \frac{1}{32\pi^2 Q^4} \int d^2\mathbf{k}_{1\perp} d^2\mathbf{k}_{2\perp} \frac{d^2\mathbf{k}'_{1\perp}}{(2\pi)^2} \delta^{(2)}(\mathbf{q}_\perp - \mathbf{k}_{1\perp} - \mathbf{k}_{2\perp}) e^{i(\mathbf{k}_{1\perp} - \mathbf{k}'_{1\perp}) \cdot \mathbf{b}_\perp} \\ &\times \left\{ \cos(\phi_1 - \phi_2) \cos(\phi'_1 - \phi'_2) |M_{++}|^2 + \cos(\phi_1 + \phi_2) \cos(\phi'_1 + \phi'_2) |M_{+-}|^2 \right. \\ &\quad \left. - \cos(\phi_1 + \phi_2) \cos(\phi'_1 - \phi'_2) M_{++} M_{+-}^* - \cos(\phi_1 - \phi_2) \cos(\phi'_1 + \phi'_2) M_{+-} M_{++}^* \right\} \\ &\times \mathcal{F}(x_1, \mathbf{k}_{1\perp}^2) \mathcal{F}^*(x_1, \mathbf{k}'_{1\perp}^2) \mathcal{F}(x_2, \mathbf{k}_{2\perp}^2) \mathcal{F}^*(x_2, \mathbf{k}'_{2\perp}^2), \end{aligned} \quad (2)$$

where $y_{1,2}$ denote the rapidities of the outgoing photon and J/ψ , connected with the incident photons' longitudinal momentum fractions $x_{1,2}$ via $x_{1,2} = \frac{1}{\sqrt{s}}(m_\perp e^{\pm y_1} + P_\perp e^{\pm y_2})$ for $J/\psi + \gamma$ and $x_{1,2} = \frac{m_\perp}{\sqrt{s}}(e^{\pm y_1} +$

$e^{\pm y_2})$ for $J/\psi + J/\psi$.

$e^{\pm y_2})$ for $J/\psi + J/\psi$, where $m_\perp = \sqrt{P_\perp^2 + m_{J/\psi}^2}$ denotes the transverse mass of the J/ψ . (\sqrt{s} denotes the center-of-mass energy of each nucleon pair from the colliding nuclei). $\phi_{1,2}$ signify the azimuthal angles between $\mathbf{k}_{1,2\perp}$ and \mathbf{P}_\perp . $\mathbf{k}'_{1,2\perp}$ denote the transverse momenta of the incoming photons in the conjugated production amplitude, with $\phi'_{1,2}$ denoting the azimuthal angles between $\mathbf{k}'_{1,2\perp}$ and \mathbf{P}_\perp ².

The nonperturbative distribution function $\mathcal{F}(x, \mathbf{k}_\perp^2)$ in Eq. (2) characterizes the probability amplitude for finding a photon that carries the prescribed light-momentum fraction and transverse momenta inside a lead nucleus. It is intimately related to the standard photon TMD parton distribution functions (PDFs) of a heavy nucleus:

$$\begin{aligned} & \int \frac{dy^- d^2 y_\perp}{P^+(2\pi)^3} e^{ik \cdot y} \langle A | F_{+\perp}^\mu(0) F_{+\perp}^\nu(y) | A \rangle \Big|_{y^+=0} \\ &= \frac{\delta_\perp^{\mu\nu}}{2} x f_1(x, \mathbf{k}_\perp^2) + \left(\frac{k_\perp^\mu k_\perp^\nu}{\mathbf{k}_\perp^2} - \frac{\delta_\perp^{\mu\nu}}{2} \right) x h_1^\perp(x, \mathbf{k}_\perp^2), \end{aligned} \quad (3)$$

where f_1 and h_1^\perp signify the unpolarized and linearly-polarized photon TMD distributions, respectively. The transverse metric tensor in (3) is defined by $\delta_\perp^{\mu\nu} = -g^{\mu\nu} + \frac{P^\mu n^\nu + P^\nu n^\mu}{P \cdot n}$ with $n^\mu = (1, -1, 0, 0)/\sqrt{2}$, and $k_\perp^2 = \delta_\perp^{\mu\nu} k_{\perp\mu} k_{\perp\nu}$. At small x , the TMD PDFs f_1 and h_1^\perp are simply identified with the square of \mathcal{F} [9, 10]:

$$x f_1(x, \mathbf{k}_\perp^2) = x h_1^\perp(x, \mathbf{k}_\perp^2) = |\mathcal{F}(x, \mathbf{k}_\perp^2)|^2. \quad (4)$$

In our actual numerical calculation, $\mathcal{F}(x, \mathbf{k}_\perp^2)$ is determined by the Woods-Saxon distribution which is taken from [23].

For later use, let us specify the polarization vectors of the photon with definite helicities:

$$\epsilon^\mu(k_1, \pm) = \frac{1}{\sqrt{2}}(0, \mp 1, -i, 0). \quad (5)$$

One can define the polarization vector of the second photon to be $\epsilon^\mu(k_2, \pm) = \epsilon^\mu(k_1, \mp)$, following Jacob-Wick's second particle phase convention [79].

When evaluating the helicity amplitudes, it is constructive to reexpress the rank-2 tensors in (3) in

terms of the photon's polarization vectors [78]:

$$\delta_\perp^{\mu\nu} = \epsilon^\mu(k_i, +) \epsilon^\nu(k_i, -) + \epsilon^\nu(k_i, +) \epsilon^\mu(k_i, -), \quad (6a)$$

$$\begin{aligned} \delta_\perp^{\mu\nu} - 2 \frac{k_{i\perp}^\mu k_{i\perp}^\nu}{k_{i\perp}^2} \\ = e^{2i\phi_i} \epsilon^\mu(k_i, +) \epsilon^\nu(k_i, +) + e^{-2i\phi_i} \epsilon^\mu(k_i, -) \epsilon^\nu(k_i, -), \end{aligned} \quad (6b)$$

with $i = 1, 2$. For definiteness, we have chosen \mathbf{P}_\perp to align with the \hat{x} -axis, and ϕ_1 and ϕ_2 represent the azimuthal angles between $\mathbf{k}_{1\perp}$, $\mathbf{k}_{2\perp}$ and \mathbf{P}_\perp .

The coefficient M_{λ_1, λ_2} in Eq. (2) denotes the helicity amplitude for the partonic reactions $\gamma(x_1 P, \lambda_1) \gamma(x_2 \bar{P}, \lambda_2) \rightarrow J/\psi(p_1) + \gamma(J/\psi)(p_2)$. $M_{\lambda_1, \lambda_2} M_{\lambda'_1, \lambda'_2}^*$ in Eq. (2) signifies a shorthand for the interference between one helicity amplitude with another conjugated one, which bear different photons' helicity configurations, yet with all the polarizations of the final-state particles (J/ψ polarizations $\lambda_{3,4} = 0, \pm 1$ and photon helicity $\lambda_4 = \pm 1$) summed over:

$$M_{\lambda_1, \lambda_2} M_{\lambda'_1, \lambda'_2}^* = \sum_{\lambda_3} \sum_{\lambda_4} M_{\lambda_1, \lambda_2, \lambda_3, \lambda_4} M_{\lambda'_1, \lambda'_2, \lambda_3, \lambda_4}^*. \quad (7)$$

Note that the transverse momenta of the incoming photons have been set to zero when calculating the helicity amplitudes, in line with the spirit of TMD factorization. Parity invariance has been invoked to reduce the number of encountered helicity configurations of incoming photons in Eq. (2).

We evaluate all the encountered helicity amplitudes within the NRQCD factorization approach [74]. At LO in the strong coupling α_s and velocity expansion, the calculation can be facilitated by using the covariant projector approach by replacing J/ψ with a comoving color-singlet $c\bar{c}$ pair carrying the quantum number 3S_1 . We devote Appendix A to the explicit expressions of all the encountered $M_{\lambda_1, \lambda_2} M_{\lambda'_1, \lambda'_2}^*$ in this work.

Equation (2) constitutes the master formula of this work. The first two terms in the curly bracket contribute to the azimuthally averaged cross section, which differs from the expression for the azimuthally averaged cross section derived in Refs. [80–83] due to the intriguing entanglement between the impact parameter and polarization vectors of the coherent photons. More interestingly, the last two terms in the curly bracket in Eq. (2), *viz.*, the terms proportional to $M_{++} M_{+-}^*$ and $M_{+-} M_{++}^*$, entail the interference between different helicity amplitudes, which is a direct consequence of the linear polarization of the incoming quasi-real photons. After integrating over the transverse momenta of incoming photons, the angular correlations between $\mathbf{k}_{i\perp}$, $\mathbf{k}'_{i\perp}$ and \mathbf{P}_\perp in the last two terms in the curly bracket are converted into the angular correlation between \mathbf{q}_\perp and \mathbf{P}_\perp . Specifically, the interference between the unpolarized and linearly polarized photon distributions generates the $\cos(2\phi)$ asymmetry, while the interference between two linearly polarized photon distributions drives the $\cos(4\phi)$ modulation.

² The appearance of $\mathbf{k}'_{i\perp}$ arises from incorporating the impact parameter dependence into our calculation. The variable \mathbf{b}_\perp enters the cross section through the phase factor in Eq. (2). Upon integrating over \mathbf{b}_\perp in Eq. (2), the cross section, which depends jointly on \mathbf{b}_\perp and \mathbf{q}_\perp , reduces to the standard result obtained in TMD factorization. For example, see Ref. [78] for a related discussion in a different context, where the lead ion is replaced by a pointlike electron or positron.

III. PHENOMENOLOGY

To facilitate the comparison between experiment and theory, we define the average value of $\cos(2\phi)$ and $\cos(4\phi)$ as

$$\langle \cos(n\phi) \rangle \equiv \frac{\int d\sigma \cos(n\phi)}{\int d\sigma}, \quad (8)$$

with $n = 2, 4$.

In the numerical calculations, we adopt the following input parameters: the center-of-mass energy $\sqrt{s_{\text{NN}}} = 5.02$ TeV, the charm quark mass $m_c = 1.5$ GeV, and the Schrödinger radial wave function at the origin for the J/ψ , $|R_{J/\psi}(0)|^2 = 0.9215$ GeV³ [84]. We use the package **HOPPET** [85] to evaluate the running strong coupling constant $\alpha_s(\mu = Q/2)$ at one-loop accuracy. We also impose the following kinematic cuts: $1.6 < |y_1|, |y_2| < 2.4$, $Q < 20$ GeV, and $P_\perp > 200$ MeV. In addition, we integrate over q_\perp from 0 to 200 MeV.

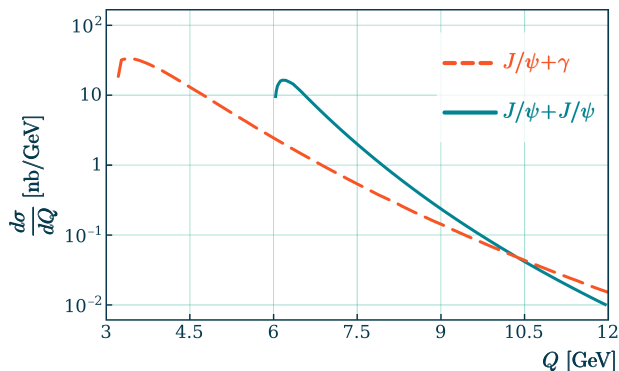


FIG. 2: The spectra of the invariant mass of $J/\psi + \gamma$ (J/ψ) for exclusive $J/\psi + \gamma$ and $J/\psi + J/\psi$ production in Pb+Pb UPCs at $\sqrt{s_{\text{NN}}} = 5.02$ TeV, under the cuts $1.6 < |y_{1,2}| < 2.4$, $P_\perp > 200$ MeV, with q_\perp integrated up to 200 MeV.

Our numerical studies indicate that the exclusive production of $J/\psi + \gamma$ and $J/\psi + J/\psi$ in Pb+Pb UPCs at $\sqrt{s_{\text{NN}}} = 5.02$ TeV yields sizable cross sections within the aforementioned kinematic constraint. As shown in Fig. 2, the differential cross sections $d\sigma/dQ$ as functions of the invariant mass Q exhibit similar behaviors for the two processes, both peaking near their respective production thresholds and decreasing with increasing Q . Remarkably, the $J/\psi + \gamma$ channel features a larger cross section, despite the nominal suppression brought by the QED fine structure constant. Concretely speaking, the integrated cross section for $J/\psi + J/\psi$ production within the prescribed kinematic window is about 13.4 nb, in contrast with 43.4 nb for $J/\psi + \gamma$ production.

We plot the azimuthal distribution $d\sigma/d\phi$ in Fig. 3. The $\cos(2\phi)$ and $\cos(4\phi)$ modulation behaviors are visible for both processes, highlighting the crucial impact of the photon linear polarization in generating these

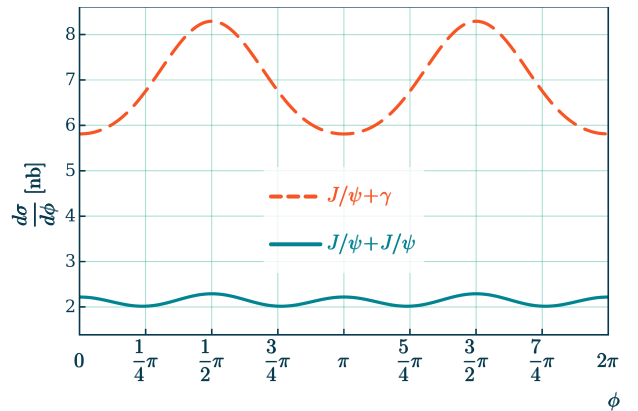


FIG. 3: The azimuthal distribution $d\sigma/d\phi$ for $J/\psi + \gamma$ (J/ψ) production in Pb+Pb UPCs at $\sqrt{s_{\text{NN}}} = 5.02$ TeV, integrated over Q from threshold to 20 GeV and q_\perp from 0 to 200 MeV, with cuts $1.6 < |y_{1,2}| < 2.4$ and $P_\perp > 200$ MeV.

angular correlations. These azimuthal asymmetries can be quantitatively visualized in Fig. 4. For both processes $\langle \cos(2\phi) \rangle$ is negative while $\langle \cos(4\phi) \rangle$ is positive. For $J/\psi + \gamma$ production, $\langle \cos(2\phi) \rangle$ dominates the asymmetry, with its absolute value exceeding 13% near the production threshold. For $J/\psi + J/\psi$ production, while $\langle \cos(4\phi) \rangle$ has a larger absolute value than $\langle \cos(2\phi) \rangle$, the maximal asymmetry reaches only about 3% near the threshold.

One may wonder how these predicted azimuthal asymmetries are influenced by radiative and relativistic corrections. Fortunately, as ratios of cross-sections, the azimuthal observables defined in Eq. 8 are expected to remain stable when higher-order corrections are included. For the same reason, we anticipate that our predictions are only mildly sensitive to the precise values of the NRQCD LDMEs, which currently carry significant uncertainties.

IV. CONCLUSION

In this paper, we have presented the first TMD factorization analysis of $J/\psi + \gamma$ and $J/\psi + J/\psi$ production in ultraperipheral Pb+Pb collisions at LHC. Taking the LO NRQCD predictions for the helicity amplitudes of $\gamma\gamma \rightarrow J/\psi + \gamma$ (J/ψ) as input, we have demonstrated that the linear polarization of quasi-real photons do induce azimuthal correlation in the final state.

Our central finding is the prediction of sizable $\cos(2\phi)$ and $\cos(4\phi)$ asymmetries, reaching up to 13% in accessible kinematic regions at the LHC. These modulations arise purely from the quantum interference between distinct photon helicity states—a phenomenon completely missed by the familiar EPA approach. The

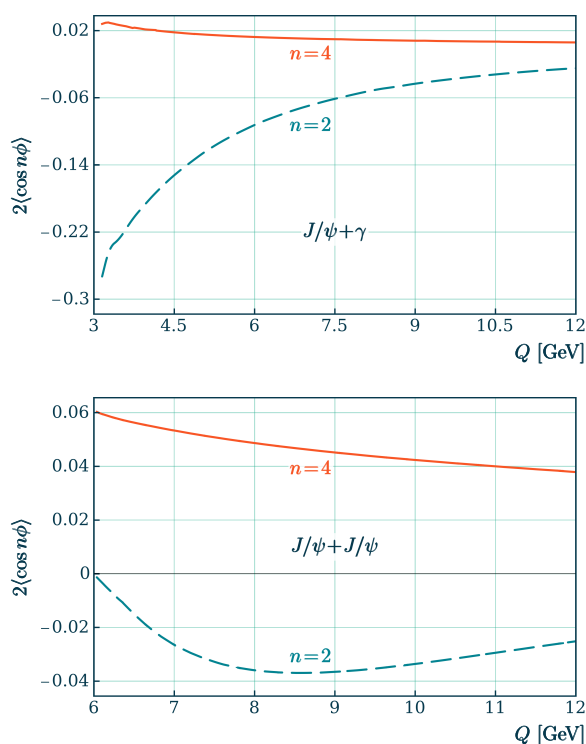


FIG. 4: The azimuthal asymmetry observables $\langle \cos(2\phi) \rangle$ and $\langle \cos(4\phi) \rangle$, as a function of the invariant mass Q for $J/\psi + \gamma$ and $J/\psi + J/\psi$ production in Pb+Pb UPCs at $\sqrt{s_{\text{NN}}} = 5.02$ TeV, under the kinematic constraints $1.6 < |y_{1,2}| < 2.4$, $Q < 20$ GeV and $P_{\perp} > 200$ MeV.

cleanliness of the UPC environment together with the clearness of the J/ψ and photon signals, ensures that these azimuthal observables can serve a novel testing ground for exclusive quarkonium production mechanism and the photon TMD structure in the ultrarelativistic limit.

As the observables built out of ratios of weighted to unweighted cross sections, these azimuthal asymmetries are expected to be largely immune to systematic uncertainties associated with integrated luminosity, the absolute normalization of NRQCD LDMEs as well as higher order corrections. Concerning the rich spin information encoded in the $\gamma\gamma \rightarrow J/\psi + \gamma(J/\psi)$ amplitudes, it appears interesting to further investigate the azimuthal correlation for *polarized* J/ψ production in UPCs, as well as explore the quantum entanglement and spin correlation between two outgoing polarized J/ψ .

Acknowledgments

We are grateful to Shuai Yang for helpful discussions. This work was supported by the High Performance Computing Center of Central South University. The

work of Y. J. is supported in part by the NNSFC under Grant No. 12475090. The work of W. S. is supported in part by the NNSFC under Grant No. 12375079. The work of X. X. is supported in part by the NNSFC under Grant No. 12275364. The work of J. Z. is supported in part by the NNSFC under Grant No. 12175118 and No. 12321005. The work of Y. Z. is supported in part by the NNSFC (Grants No. 12475084) and the Natural Science Foundation of Shandong Province (Grant No. ZR2024MA012).

Appendix A: Squared Helicity Amplitudes for $\gamma\gamma \rightarrow J/\psi + \gamma(J/\psi)$

In this appendix, we present explicit expressions for the interference of one helicity amplitude with another conjugated one, *viz.*, $M_{\lambda_1, \lambda_2} M_{\lambda'_1, \lambda'_2}^*$ in Eq. (2). The helicity amplitudes are projected from the LO NRQCD predictions for the $\gamma\gamma \rightarrow J/\psi + \gamma(J/\psi)$ amplitudes. These squared helicity amplitudes depend upon the Mandelstam variables s, t, u and charm quark mass m_c , as well as upon the lowest-order NRQCD LDME of J/ψ , often approximated by the wave function at the origin for J/ψ .

For the $\gamma\gamma \rightarrow J/\psi + \gamma$ reaction, the three independent squared helicity amplitudes read

$$|M_{++}|^2 = \mathcal{N}_1 \frac{s^2}{(s+t)^2(s+u)^2}, \quad (\text{A1a})$$

$$|M_{+-}|^2 = \mathcal{N}_1 \frac{s^2(t^2+u^2) + 2stu(t+u) + 2t^2u^2}{(s+t)^2(s+u)^2(t+u)^2}, \quad (\text{A1b})$$

$$M_{++} M_{+-}^* = M_{+-} M_{++}^* = \mathcal{N}_1 \frac{4m_c^2 s t u}{(s+t)^2(s+u)^2(t+u)^2}, \quad (\text{A1c})$$

where the normalization factor $\mathcal{N}_1 = 24576 \pi^2 \alpha^3 e_c^6 m_c |R_{J/\psi}(0)|^2$, with α the QED coupling constant and $e_c = 2/3$.

For the $\gamma\gamma \rightarrow J/\psi + J/\psi$ channel, the results become more involved relative to the $J/\psi + \gamma$ production, due to the presence of the extra gluon exchange. The three independent squared helicity amplitudes read

$$|M_{++}|^2 = \mathcal{N}_2 (s - 12m_c^2)(s - 4m_c^2) \left[\frac{s^3}{(t - 4m_c^2)^4} + \frac{2s}{(t - 4m_c^2)^2} - \frac{4}{t - 4m_c^2} + \left(t \leftrightarrow u \right) \right], \quad (\text{A2a})$$

$$|M_{+-}|^2 = \mathcal{N}_2 \left[\frac{16m_c^2 s^3}{(t - 4m_c^2)^3} + \frac{s^3(4m_c^2 + s)(12m_c^2 + s)}{(t - 4m_c^2)^4} + \frac{2s(4m_c^2 + s)(12m_c^2 + 5s)}{(t - 4m_c^2)^2} \right. \\ \left. + \frac{1}{32}s \left(\frac{s^2}{m_c^4} - \frac{16s}{m_c^2} + 192 \right) - \frac{192m_c^6 + 32m_c^4s + s^3}{m_c^2(t - 4m_c^2)} + \left(t \leftrightarrow u \right) \right], \quad (\text{A2b})$$

$$M_{++} M_{+-}^* = M_{+-} M_{++}^* = \mathcal{N}_2 \left[\frac{s(-96m_c^4 - 16m_c^2s + s^2)}{(t - 4m_c^2)^2} - \frac{8m_c^2 s^3}{(t - 4m_c^2)^3} - \frac{16m_c^2(s - 12m_c^2)}{t - 4m_c^2} - \frac{48m_c^4 s^3}{(t - 4m_c^2)^4} \right. \\ \left. + \left(t \leftrightarrow u \right) \right], \quad (\text{A2c})$$

where the normalization factor $\mathcal{N}_2 = \frac{4194304 \pi^2 \alpha_s^2 \alpha^2 e_c^4 m_c^2 |R_{J/\psi}(0)|^4}{9s^5}$.

[1] J. Adam et al. (STAR), Phys. Rev. Lett. **127**, 052302 (2021), 1910.12400.

[2] S. Acharya et al. (ALICE), Phys. Lett. B **798**, 134926 (2019), 1904.06272.

[3] S. Acharya et al. (ALICE), JHEP **06**, 035 (2020), 2002.10897.

[4] S. Acharya et al. (ALICE), Eur. Phys. J. C **81**, 712 (2021), 2101.04577.

[5] E. Abbas et al. (ALICE), Eur. Phys. J. C **73**, 2617 (2013), 1305.1467.

[6] A. M. Sirunyan et al. (CMS), Phys. Rev. Lett. **127**, 122001 (2021), 2011.05239.

[7] G. Aad et al. (ATLAS), Phys. Rev. C **104**, 024906 (2021), 2011.12211.

[8] M. Abdallah et al. (STAR), Sci. Adv. **9**, eabq3903 (2023), 2204.01625.

[9] C. Li, J. Zhou, and Y.-J. Zhou, Phys. Rev. D **101**, 034015 (2020), 1911.00237.

[10] C. Li, J. Zhou, and Y.-J. Zhou, Phys. Lett. B **795**, 576 (2019), 1903.10084.

[11] Y. Hagiwara, C. Zhang, J. Zhou, and Y.-J. Zhou, Phys. Rev. D **103**, 074013 (2021), 2011.13151.

[12] Y. Hagiwara, C. Zhang, J. Zhou, and Y.-J. Zhou, Phys. Rev. D **104**, 094021 (2021), 2106.13466.

[13] H. Xing, C. Zhang, J. Zhou, and Y.-J. Zhou, JHEP **10**, 064 (2020), 2006.06206.

[14] H. Mäntysaari, F. Salazar, B. Schenke, C. Shen, and W. Zhao, Phys. Rev. C **109**, 024908 (2024), 2310.15300.

[15] H. Mäntysaari, F. Salazar, and B. Schenke, Phys. Rev. D **106**, 074019 (2022), 2207.03712.

[16] J. D. Brandenburg, H. Duan, Z. Tu, R. Venugopalan, and Z. Xu (2024), 2407.15945.

[17] S. Lin, J.-Y. Hu, H.-J. Xu, S. Pu, and Q. Wang (2024), 2405.16491.

[18] D. Y. Shao, Y. Shi, C. Zhang, J. Zhou, and Y.-J. Zhou, JHEP **07**, 189 (2024), 2402.05465.

[19] Y. Hagiwara, Y. Hatta, R. Pasechnik, M. Tasevsky, and O. Teryaev, Phys. Rev. D **96**, 034009 (2017), 1706.01765.

[20] E. Iancu, A. H. Mueller, D. N. Triantafyllopoulos, and S. Y. Wei, Eur. Phys. J. C **83**, 1078 (2023), 2304.12401.

[21] P.-Y. Niu, E. Wang, Q. Wang, and S. Yang (2022), 2209.01924.

[22] J. Jiang, S.-Y. Li, X. Liang, Y.-R. Liu, C.-F. Qiao, Z.-G. Si, and H. Yang (2024), 2406.19735.

[23] S. R. Klein, J. Nystrand, J. Seger, Y. Gorbunov, and J. Butterworth, Comput. Phys. Commun. **212**, 258 (2017), 1607.03838.

[24] C. A. Bertulani and G. Baur, Phys. Rept. **163**, 299 (1988).

[25] C. A. Bertulani, S. R. Klein, and J. Nystrand, Ann. Rev. Nucl. Part. Sci. **55**, 271 (2005), nucl-ex/0502005.

[26] A. J. Baltz, Phys. Rept. **458**, 1 (2008), 0706.3356.

[27] J. Zhao, J.-H. Chen, X.-G. Huang, and Y.-G. Ma, Nucl. Sci. Tech. **35**, 20 (2024), 2211.03968.

[28] P. Copinger, K. Fukushima, and S. Pu, Phys. Rev. Lett. **121**, 261602 (2018), 1807.04416.

[29] S. Klein, A. Mueller, B.-W. Xiao, and F. Yuan, Phys. Rev. Lett. **122**, 132301 (2019), 1811.05519.

[30] S. Klein, A. Mueller, B.-W. Xiao, and F. Yuan (2020), 2003.02947.

[31] D. Y. Shao, C. Zhang, J. Zhou, and Y.-j. Zhou, Phys. Rev. D **108**, 116015 (2023), 2306.02337.

[32] D. Y. Shao, C. Zhang, J. Zhou, and Y.-J. Zhou, Phys. Rev. D **107**, 036020 (2023), 2212.05775.

[33] J.-Y. Hu, S. Lin, S. Pu, and Q. Wang (2024), 2407.06091.

[34] C. Zhang, L.-M. Zhang, and D. Y. Shao (2024), 2406.05618.

[35] K. Hencken, G. Baur, and D. Trautmann, Phys. Rev. C **69**, 054902 (2004), nucl-th/0402061.

[36] W. Zha, J. D. Brandenburg, Z. Tang, and Z. Xu, Phys. Lett. B **800**, 135089 (2020), 1812.02820.

[37] J. D. Brandenburg, W. Zha, and Z. Xu, Eur. Phys. J. A **57**, 299 (2021), 2103.16623.

[38] B.-W. Xiao, F. Yuan, and J. Zhou (2020), 2003.06352.

[39] R.-j. Wang, S. Pu, and Q. Wang, Phys. Rev. D **104**, 056011 (2021), 2106.05462.

[40] R.-j. Wang, S. Lin, S. Pu, Y.-f. Zhang, and Q. Wang, Phys. Rev. D **106**, 034025 (2022), 2204.02761.

[41] S. Lin, R.-J. Wang, J.-F. Wang, H.-J. Xu, S. Pu, and Q. Wang, Phys. Rev. D **107**, 054004 (2023), 2210.05106.

[42] D. Y. Shao, H.-Q. Yu, C. Zhang, and J. Zhou (2025), 2511.17670.

[43] I. Xu, N. Lewis, X. Wang, J. D. Brandenburg, and L. Ruan (2022), 2211.02132.

[44] D. Shao, B. Yan, S.-R. Yuan, and C. Zhang, Sci. China Phys. Mech. Astron. **67**, 281062 (2024), 2310.14153.

[45] A. Metz and J. Zhou, Phys. Rev. D **84**, 051503 (2011), 1105.1991.

[46] J. P. Ma, J. X. Wang, and S. Zhao, Phys. Lett. B **737**, 103 (2014), 1405.3373.

[47] G.-P. Zhang, Phys. Rev. D **90**, 094011 (2014), 1406.5476.

[48] J. P. Ma and C. Wang, Phys. Rev. D **93**, 014025 (2016), 1509.04421.

[49] D. Boer, P. J. Mulders, C. Pisano, and J. Zhou, JHEP **08**, 001 (2016), 1605.07934.

[50] D. Boer, P. J. Mulders, J. Zhou, and Y.-j. Zhou, JHEP **10**, 196 (2017), 1702.08195.

[51] J.-P. Lansberg and H.-S. Shao, EPJ Web Conf. **137**, 06013 (2017), 1611.10306.

[52] G.-P. Zhang, JHEP **11**, 069 (2017), 1709.08970.

[53] J.-P. Lansberg, C. Pisano, F. Scarpa, and M. Schlegel, Phys. Lett. B **784**, 217 (2018), [Erratum: Phys.Lett.B 791, 420–421 (2019)], 1710.01684.

[54] A. Bacchetta, D. Boer, C. Pisano, and P. Taels, Eur. Phys. J. C **80**, 72 (2020), 1809.02056.

[55] F. Scarpa, D. Boer, M. G. Echevarria, J.-P. Lansberg, C. Pisano, and M. Schlegel, Eur. Phys. J. C **80**, 87 (2020), 1909.05769.

[56] D. Boer, U. D'Alesio, F. Murgia, C. Pisano, and P. Taels, JHEP **09**, 040 (2020), 2004.06740.

[57] R. Kishore, A. Mukherjee, and M. Siddiqah, Phys. Rev. D **104**, 094015 (2021), 2103.09070.

[58] P. Taels, T. Altinoluk, G. Beuf, and C. Marquet, JHEP **10**, 184 (2022), 2204.11650.

[59] H. liu, X. xie, and Z. Lu, Phys. Lett. B **849**, 138439 (2024), 2310.00609.

[60] P. Caucal, F. Salazar, B. Schenke, T. Stobel, and R. Venugopalan, Phys. Rev. Lett. **132**, 081902 (2024), 2308.00022.

[61] L. Maxia and F. Yuan, Phys. Rev. D **110**, 114042 (2024), 2403.02097.

[62] Z.-Q. Chen and L.-B. Chen, Phys. Rev. D **112**, 056013 (2025), 2508.06946.

[63] W. J. den Dunnen, J. P. Lansberg, C. Pisano, and M. Schlegel, Phys. Rev. Lett. **112**, 212001 (2014), 1401.7611.

[64] L. Alimov, A. Karpishkov, and V. Saleev, Int. J. Mod. Phys. A **40**, 2550020 (2025), 2412.01710.

[65] Y. Hatta, B.-W. Xiao, F. Yuan, and J. Zhou, Phys. Rev. D **104**, 054037 (2021), 2106.05307.

[66] Y. Hatta, B.-W. Xiao, F. Yuan, and J. Zhou, Phys. Rev. Lett. **126**, 142001 (2021), 2010.10774.

[67] C.-F. Qiao, Phys. Rev. D **64**, 077503 (2001), hep-ph/0104309.

[68] S. Baranov, A. Cisek, M. Klusek-Gawenda, W. Schafer, and A. Szczurek, Eur. Phys. J. C **73**, 2335 (2013), 1208.5917.

[69] H. Yang, Z.-Q. Chen, and C.-F. Qiao (2020), 2006.05351.

[70] H. Yang, Z.-Q. Chen, and C.-F. Qiao, Eur. Phys. J. C **80**, 806 (2020).

[71] Z.-G. He, X.-B. Jin, B. A. Kniehl, and R. Li, Chin. Phys. C **48**, 083107 (2024), 2404.08945.

[72] H. Yang, Z.-Q. Chen, and B. Long, Eur. Phys. J. C **85**, 802 (2025), 2504.14850.

[73] M.-K. Jia, X.-B. Jin, K.-Y. Liu, and G.-Z. Xu (2025), 2510.10318.

[74] G. T. Bodwin, E. Braaten, and G. P. Lepage, Phys. Rev. D **51**, 1125 (1995), [Erratum: Phys.Rev.D 55, 5853 (1997)], hep-ph/9407339.

[75] M. Vidovic, M. Greiner, C. Best, and G. Soff, Phys. Rev. C **47**, 2308 (1993).

[76] K. Hencken, D. Trautmann, and G. Baur, Phys. Rev. A **51**, 1874 (1995), nucl-th/9410014.

[77] Y. Jia, S. Lin, J. Zhou, and Y.-j. Zhou (2024), 2410.13781.

[78] Y. Jia, J. Zhou, and Y.-j. Zhou, Phys. Rev. Lett. **134**, 141901 (2025), 2406.09381.

[79] H. E. Haber, in *21st Annual SLAC Summer Institute on Particle Physics: Spin Structure in High-energy Processes (School: 26 Jul - 3 Aug, Topical Conference: 4-6 Aug) (SSI 93)* (1994), pp. 231–272, hep-ph/9405376.

[80] M. Klusek-Gawenda, P. Lebiedowicz, and A. Szczurek, Phys. Rev. C **93**, 044907 (2016), 1601.07001.

[81] L. A. Harland-Lang, M. Tasevsky, V. A. Khoze, and M. G. Ryskin, Eur. Phys. J. C **80**, 925 (2020), 2007.12704.

- [82] H.-S. Shao and D. d'Enterria, JHEP **09**, 248 (2022), 2207.03012.
- [83] A. A H, E. Chaubey, M. Fraaije, V. Hirschi, and H.-S. Shao, Phys. Lett. B **851**, 138555 (2024), 2312.16956.
- [84] G. T. Bodwin, J. Lee, and C. Yu, Phys. Rev. D **77**, 094018 (2008), 0710.0995.
- [85] A. Karlberg, P. Nason, G. Salam, G. Zanderighi, and F. Dreyer (2025), 2510.09310.